Robotica (2023), **41**, pp. 2774–2788
doi:10.1017/S026357472300067X

CAMBRIDGE UNIVERSITY PRESS

RESEARCH ARTICLE

Design and characterisation of a multi-DOF soft pneumatic module

Israel Santacruz-Mondragon[1,2], X. Yamile Sandoval-Castro[3], Serhat Ibrahim[4], Mats Wiese[4], Annika Raatz[4], Maximiano F. Ruiz-Torres[1] and Eduardo Castillo-Castaneda[1]

[1]Instituto Politécnico Nacional, CICATA Unidad Querétaro, Mexico, [2]Mechatronics Engineering, Universidad Anáhuac Querétaro, Querétaro, Mexico, [3]Department of Mechatronics, CONACYT-IPN, Querétaro, Mexico, and [4]Leibniz University Hannover, Institute of Assembly Technology, Hannover, Germany
Corresponding authors: Israel Santacruz-Mondragon, X. Yamile Sandoval-Castro;
Emails: isra.stacruz@gmail.com, xyamile.sc@gmail.com

Received: 13 June 2022; **Revised:** 10 March 2023; **Accepted:** 19 April 2023; **First published online:** 1 June 2023

Keywords: multi-DOF soft pneumatic actuator; Ecoflex-0050; wide range of mobility; characterisation; kinematics; soft manipulation; manipulation applications

Abstract

Bending and elongation have been some of the most studied motions in soft actuators due to the variety of their applications. For that matter, multi-DOF actuators have been developed with the purpose to generate different movements in a single actuator, mainly bending.
However, these actuators are still limited in mobility range, and some of them do not perform continuous curvatures. This paper presents the design, characterisation and implementations of a multi-DOF soft pneumatic module. The internal structure of the proposed module is composed of four channels, which generate bending in several directions. The finite element method analysis demonstrates that the actuator performs continuous curvatures for different pressure values. We present a repeatable and easy manufacturing process using the casting technique, considering the material Ecoflex 00-50; as well as the kinematic model of the actuator, taking into consideration two bending Degrees of Freedom (DOFs). Furthermore, we performed bending characterisation for all possible combinations of the four channels via computer vision, demonstrating a wide mobility range and performing continuous curvatures. Additionally, we evaluated the kinematic model with characterisation data, obtaining the angular and cartesian relationship between the pressure and continuous curvatures. On the other hand, the authors propose the design of a modular soft manipulator based on two multi-DOF modules. The kinematic model is reported. In addition, we implement a motion sequence in the manipulator to pick and place tasks.

1. Introduction

Soft robotics has been an emerging field in recent years, and its construction is mainly based on flexible elements that provide numerous advantages. These flexible elements adapt to surfaces, distribute stress over a larger volume and increase contact time, lowering the maximum impact force [1]. Therefore, soft elements have been applied in different robotic's areas such as locomotion [2–4], exploration [5, 6], manipulation [7–9], medical and rehabilitation applications [10–12], among others.

In most cases, soft robots are conformed by a set of single motion soft actuators interconnected by themselves [13], producing structures with high dimensions and impractical geometries. Generally, soft robots are designed by actuators that generate single motion such as elongation, contracting, bending or twisting [11, 14]. The internal structure of a single motion pneumatic actuator commonly consists of chambers or channels [11, 15, 16].

Studying actuators with multiple motions remains a challenge due to the complexity of implementing multiple movements in a single structure. The technique most commonly used for the development of these multiple movement actuators is casting because it allows the manufacture of bigger actuators

than 3D printing technology, as well as more complex geometries using elastomers. An alternative to generating more than one motion in a single actuator is to place two actuators in an antagonistic way so that bending can be obtained in two directions [17, 18]. However, when more motions are necessary, this method becomes unpractical due to the complexity of joining more than two actuators. Multiple motions soft actuators have been proposed [19–24] considering chambers or at least three independent channels, distributed homogeneously in the body, resulting in motions of elongation and multiple bending and performing deformations from 36° to less than 160° [19, 21–26] (depending on the angle measurement method). The motion variation depends on the method of measurement, manufacturing material and actuator geometry. In addition, the performed motion is related to the activation of the chamber or channels, independently or simultaneously.

Different applications of soft robotics require a wide range of motion and multiple movements, mainly bending and elongation. Further, multiple-DOF actuators decrease the number of interconnected actuators in a robot. For example, the "dexterouse" gripper [27] could reduce the number of bending actuators to just one with multiple movements, allowing to reduce the total weight and dimensions. Therefore, these types of actuators increase the mobility in robotics applications [25]. Multi-motion or multi-DOF soft actuators allow modularising, which is relevant for soft manipulators and bio-inspired soft robots.

One of the most attractive applications of the multi-DOF modules is soft manipulation. In ref. [7], the authors presented a soft robot based on multi-DOF modules composed of three cavities. However, they don't approach manipulation tasks. In ref. [8], the authors presented a soft robot based on four multi-DOF modules with different configurations. They showed the end effector positioning, but not grasping and object manipulation.

This article presents the design, finite element method (FEM) simulations, manufacturing and characterisation of a multi-DOF soft pneumatic module as well as its implementation in the development of a soft manipulator.

The internal structure of the module consists of four channels. When those channels are pressurised simultaneously, elongation is achieved. Furthermore, when one channel is activated independently or two or three channels are activated synchronously, the bending motion is performed in several directions.

On the other hand, we report the manufacturing process by casting technique using the elastomer Ecoflex 00-50 supplied by Smooth On Inc. In addition to that, the characterisation of the bending motion is presented.

We report the kinematic model for the multi-DOF module as a function of the joint variables (displacement length of the four pneumatic channels) considering the curvature radius.

Finally, we present the development of a soft manipulator based on two multi-DOF soft modules. We achieved a kinematic model for a "n" number of these modules, considering the kinematic model of a single multi-DOF soft module. We manufactured the manipulator using Ecoflex 00-50. Furthermore, we present a manipulation motion sequence for picking and placing a rigid object.

2. Multi-DOF soft pneumatic module

2.1. Description of the module

For developing the multi-DOF soft pneumatic module, we define a simple geometry as a design requirement; in this way, the design, simulation and manufacturing process would be practical and efficient; therefore, it is an attractive alternative for use in robotics applications and soft manipulators. Likewise, it must have a wide range of mobility, as well as a length of 100–150 mm and a diameter of 40–70 mm. Thus, the proposed module is composed of four semicircular channels denoted by Ch_1, Ch_2, Ch_3 and Ch_4 that are controlled by independent pneumatic signals. The channels are symmetrically distributed and separated 90° around Z axis as shown in Fig. 1(b). The design of this soft pneumatic module proposes to remove the material in the central part, allowing to optimise the channels' design. The empty central part is sealed with covers, thus containing a volume of air inside. This strategy accordingly allows improved mobility because it reduces weight and the air contained inside works as an additional wall that amplifies mobility. Likewise, its peculiar geometry eliminates excess material in the module, reducing its size and weight and thus improving its performance. The module's dimensions are 47 mm wide

https://doi.org/10.1017/S026357472300067X Published online by Cambridge University Press

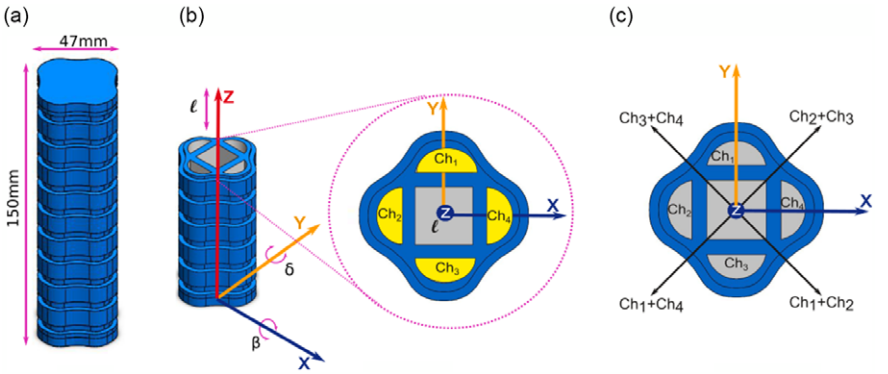

Figure 1. *Mutli-DOF soft pneumatic module description.*

by 150 mm long, the channels' wall thickness are 3 mm, while the wall thickness of central part has 3 mm (Fig. 1(a)). This module addresses a wide mobility range since the multi-channel structure allows performing bending motion in several directions as well elongation motion in the longitudinal axis direction. The independent activation of Ch_1 or Ch_3 produces bending that could be regarded as a rotation around X-axis, while the independent activation of Ch_2 or Ch_4 produces bending motion regarded as a rotation around Y-axis as shown in Fig. 1(b). Moreover, when two or three channels are activated simultaneously, bending motion is performed in different directions, as illustrated in Fig. 1(c). On the other hand, the simultaneous activation of the four channels generates elongation along the Z-axis as represented in Fig. 1(b).

The multi-channel soft pneumatic module has three DOFs: one elongation along Z-axis, represented by l, and the other two degrees of freedom correspond to bending motion regarded as rotations around X and Y axes, represented by β and δ, respectively, as described in Fig. 1(b).

2.2. FEM analysis

In this section, we present a FEM analysis of the multi-DOF soft module using ANSYS Workbench software. Four cases are considered: Ch_1 activation (Case 1), Ch_1+Ch_2 activation (Case 2), and Ch_1+Ch_2+Ch_3 activation (Case 3); these cases are for bending motion. Finally, Ch_1+Ch_2+Ch_3+Ch_4 activation (Case 4), this case generates linear displacement. However, it was performed a small linear displacement of 14.75 mm; for kinematics, we despise this motion.

The FEM analysis was performed considering the Ecoflex 00-50 as the actuator's material, which Yeoh's hyperelastic model was reported by ref. [28]. On the other hand, it is considered as boundary conditions the gravity force (G) and as a restriction the actuator has a fixed support in one of its faces (Fig. 2(a)).

For calculating the deformation angle, a coordinate system was placed on a finite element located at a point of interest in the upper part of the actuator, as shown in Fig. 2(b)). Subsequently, it is obtained its nodal coordinates from its initial state to its final state. In this way, we determine the actuator's strain-stress, reaching angles of 124.5°, 116.7° and 29.36° when activating the channels Ch_1, Ch_1+Ch_2, Ch_1+Ch_2+Ch_3, respectively. Finally, to determine the angle, the Eq. (13) and the coordinates obtained previously are used to calculate the deformation. For more information, see Section 3.1. Kinematic model.

2.3. Manufacturing process

This section presents the manufacturing process by using the casting technique. We used the elastomer Ecoflex 00-50 supplied by Smooth On, Inc., which has an elongation at break of 980% and a shore hardness of 00-50.

https://doi.org/10.1017/S026357472300067X Published online by Cambridge University Press

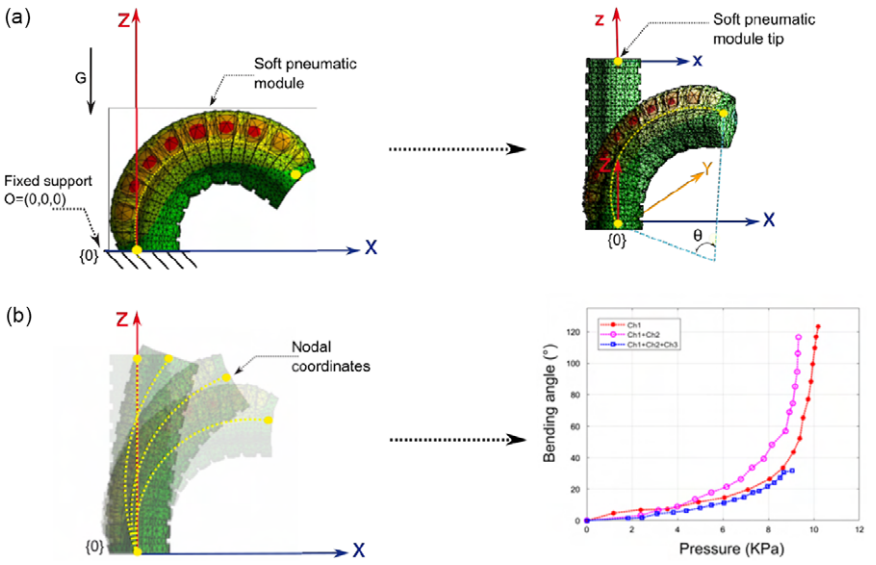

Figure 2. *FEM analysis, boundary conditions and the graphic of bending angle – pressure relationship for Ch_1, $Ch_1 + Ch_2$ and $Ch_1 + Ch_2 + Ch_3$.*

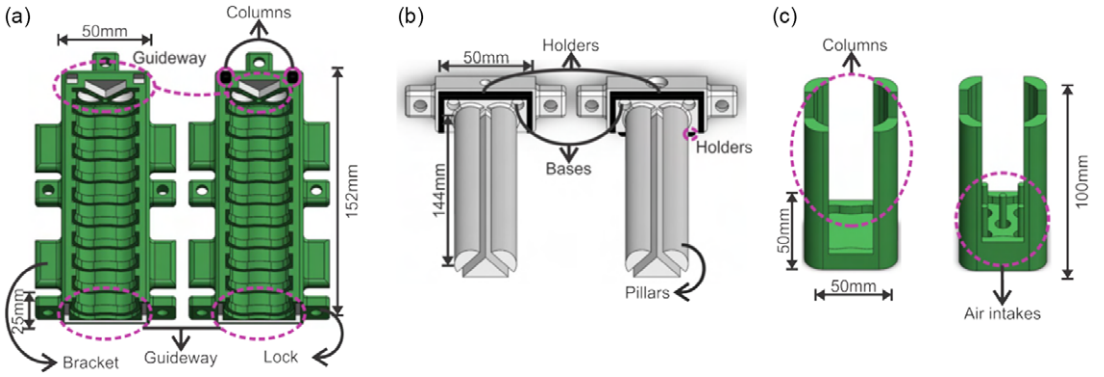

Figure 3. *Description of the moulds to manufacture the soft module: (a) main moulds, (b) channel moulds and (c) cover moulds.*

As shown in Fig. 3, we design three pairs of moulds: main moulds, channel moulds and cover moulds.

The main moulds shape the external geometry of the module (Fig. 3(a)). The length and width of these moulds are 152 and 50 mm, respectively. The columns in the mould on the right allow it to be assembled to the other main mould via the guideway. The guideway in both moulds avoid leaks in the casting process and non-alignment during assembling. Furthermore, the locks keep both moulds fixed, improving the assembly quality. The brackets permit an easy disassemble.

The channel mould illustrated in Fig. 3(b) creates the internal geometry of the module. The dimensions are length = 144 mm and width = 50 mm. The pillars are attached to the upper guideways of the main moulds, and the channel mould holders fit into the bottom guideways of the main moulds, preventing material leaks. The bases on channel moulds delimit the covers' height (5 mm). Figure 3(c) presents the cover moulds. The mould on the left allows building the bottom cover. The mould on the right generates the top cover and the four air intakes. The columns in both moulds keep the module fixed,

https://doi.org/10.1017/S026357472300067X Published online by Cambridge University Press

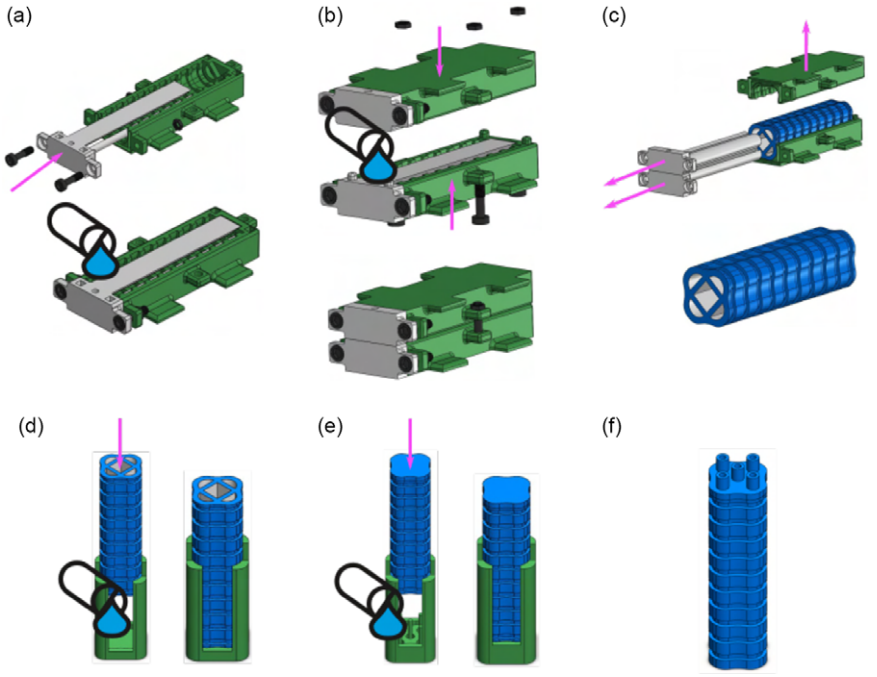

Figure 4. *Manufacturing process by casting method.*

guaranteeing appropriate sealing. The assembly of the channel mould and main mould is depicted in Fig. 4(a). In this step, the elastomer is mixed and poured into the assembled moulds. The air bubbles are eliminated by using a vacuum degasser, and afterwards the elastomer is cured for 4 h. Subsequently, step (a) is repeated with the other channel and main moulds (Fig. 4(b)). Later, both parts are assembled to shape the soft module's geometry. Again, the elastomer is cured for 4 h. In step (c), the moulds are unmounted, obtaining the module without covers. In step (d), elastomer is poured into the mould of the bottom cover. The bubbles are eliminated with the vacuum degasser, and the module generated in step (c) is assembled with this mould. Now, the elastomer is cured for 2 h. In step (e), the elastomer is poured into the mould of the top cover, generating the four air intakes and sealing the module. Here, the elastomer is cured for 2 h. Finally, in step (f), the multi-DOF soft pneumatic module is constructed.

3. Kinematics model and actuation

3.1. Kinematics model

Since the soft pneumatic module bends continuously, we seek to drive expressions for arc parameters ($l(q)$, $k(q)$, and $\phi(q)$), which represent the length of the module, the inverse of the radius of curvature r and the angle out-of-plane motion of the module, respectively. In function of the joint variables $q = [l_1, l_2, l_3, l_4]^T$ which describe the lengths of four pneumatic channels as shown in Fig. 5.

For the kinematic analysis, we consider two bending DOF. The four independent channels can be actuated with pressurised air, where the position and orientation can be controlled by programmed pressure.

Based on the work presented in ref. [29], we will now describe the kinematic model for our multi-DOF soft pneumatic module related to the curvature radius. According to Eq. (1) (Fig. 5(a)), the curvature radius r measured from the module's centre corresponds to the curvature radius for the $j-th$ channel (Fig. 5(a)):

$$r_j = r - bcos(\phi_j) \tag{1}$$

https://doi.org/10.1017/S026357472300067X Published online by Cambridge University Press

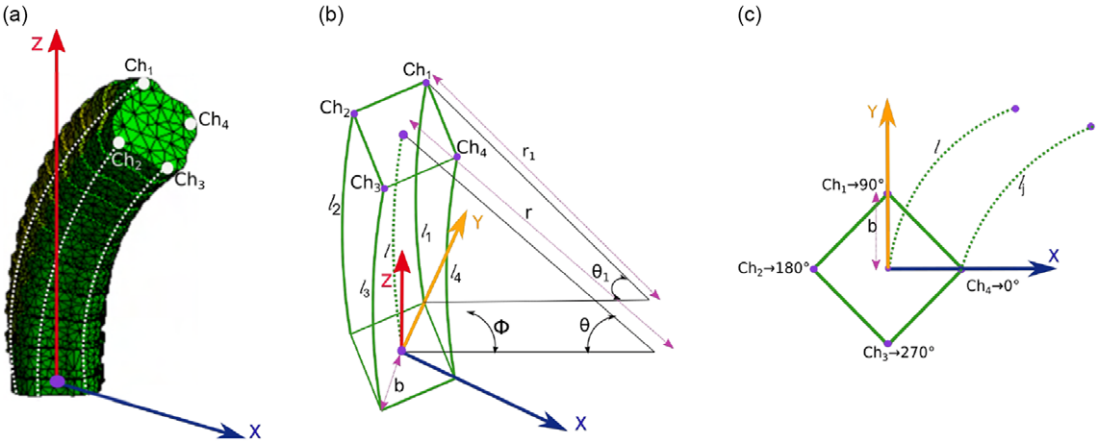

Figure 5. *(a) Diagram of a bending module related to the arc parameter. (b) Diagram of the distribution of the for channels in a single bending module, seen from top view.*

Here, b denotes the distance of a channel from the centre of the module and ϕ specifies the angle between the bending direction and the location of the $j-th$ channel.

Multiplied (Eq. (1)) by the arc angle θ and remembering that $l=\theta r$ and $l_j=\theta r_j$, the result between the arc length of the module (l) and the arc length of the $j-th$ channel (l_j):

$$l = l_j + \theta b cos(\phi_j) \tag{2}$$

Thus, it is possible to determine $l(q)$ noting that the module's location is related to its bending plane $\phi(q)$ with $\phi_1=0°$, $\phi_2=90°$, $\phi_3=180°$ and $\phi_4=270°$, as shown in Fig. 5(c). Thus, $\sum_{j=1}^{4} = cos(\phi_j) = 0$

$$l(q) = \frac{1}{4}\sum_{j=1}^{4} l_j \tag{3}$$

$$l(q) = \frac{1}{4}\left(l_1 + l_2 + l_3 + l_4 + \theta b\left(cos(\phi_1) + cos(\phi_2) + cos(\phi_3)cos(\phi_4)\right)\right) \tag{4}$$

Using Eq. (2) for the channels 1 and 3, we have $l = l_1 + \theta b cos(\phi_1)$ and $l = l_3 + \theta b cos(\phi_3)$. Equating both equations, we obtain $\theta b = \dfrac{l_3 - l_1}{cos(\phi_1) - cos(\phi_3)}$. Using the same procedure for channels 2 and 4, we compute $\phi(q)$ as shown in Eq. (5):

$$\phi(q) = tan^{-1}\left(\frac{l_4 - l_2}{l_3 - l_1}\right) \tag{5}$$

To obtain the module's curvature $k(q)$, we have $\theta = kl = \dfrac{l_j}{r_j}$ and $r_j = \dfrac{l_j}{kl}=$, combining with (1)

$$k = \frac{l - l_j}{lbcos\phi_j} \tag{6}$$

$$k(q) = \frac{(l_1 - 3l_2 + l_3 + l_4)\sqrt{(l_4 - l_2)^2 + (l_3 - l_1)^2}}{b(l_1 + l_2 + l_3 + l_4)\,(l_4 - l_2)} \tag{7}$$

On the other hand, based on the work presented in ref. [30], we will now describe the kinematic model for our multi-DOF soft pneumatic module related to the curvature radius. According to the Fig. 6, the plane of the bending (ϕ) can be found by using the projection oh the position of point C on the x–y plane (Eq. (9)):

https://doi.org/10.1017/S026357472300067X Published online by Cambridge University Press

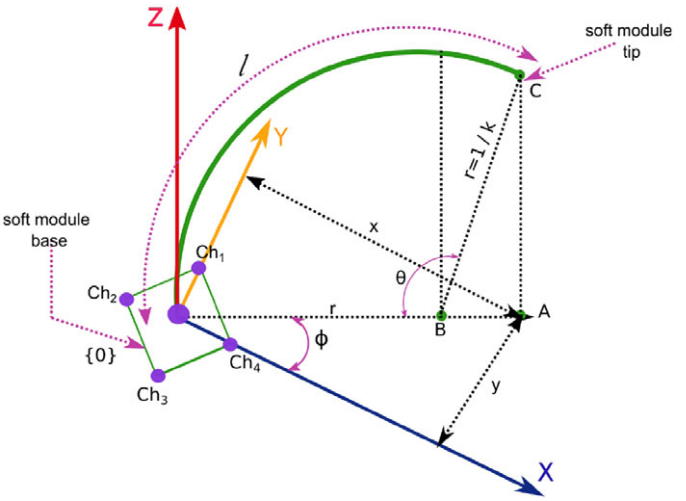

Figure 6. *Configuration of the constant curvature parameters and their relation to the fixed coordinate system.*

$$\theta = cos\left(1 - (k\sqrt{x^2 + y^2}\right) \tag{8}$$

$$\phi = tan^{-1}\left(\frac{y}{x}\right) \tag{9}$$

According to the Fig. 6 ϕ, can also be expressed as:

$$cos(\phi) = \frac{OX}{OA} = \frac{x}{\sqrt{x^2 + y^2}} \tag{10}$$

Likewise, the author [30] defines that the inverse of the radius (k) is

$$k(x, y, z) = \frac{2\sqrt{x^2 + y^2}}{x^2 + y^2 + z^2} \tag{11}$$

Also, recall that the arc length is $l = r\theta$ for the constant curvature (CC) assumption. If B is the centre of curvature, then from Fig. 6 the angle θ can be expressed as:

$$cos(\pi - \theta) = \frac{BA}{BC} = \frac{\sqrt{x^2 + y^2} - r}{r} \tag{12}$$

Rearranging and replacing r by k of the Eq. (12), then θ can be expressed as is shown in Eq. (13):

$$\theta = cos\left(1 - \left(k\sqrt{x^2 + y^2}\right)\right) \tag{13}$$

Since the proposed soft module generates constant curvatures with the multiple motions, the previously presented kinematic analysis was performed on the FEM analysis to determine the arc of curvature and its angle. In this way, it can be seen in Fig. 7(a), (b) and (c) that the multi-DOF soft module generates constant curvature when it activates Ch_1, Ch_1+Ch_2, Ch_1+Ch_2+Ch_3, respectively.

3.2. Characterisation of the multi-DOF soft pneumatic module

Sensors [31]–[32] and computer vision [14], [33], [34] are used in various characterisation methods. In this section, we present the characterisation of the multiple motion soft module through computer vision techniques. It is important to characterise the performance of soft pneumatic modules in terms of

https://doi.org/10.1017/S026357472300067X Published online by Cambridge University Press

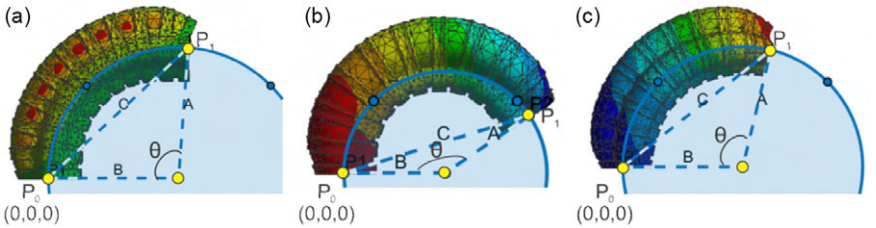

Figure 7. *Distance A = B = r. (a) Constant curvature when activating Ch_1 (θ=94°). (b) Constant curvature when activating Ch_1+Ch_2 (θ=145°). (c) Constant curvature when activating Ch_1+Ch_2+Ch_3 (θ=103.6°).*

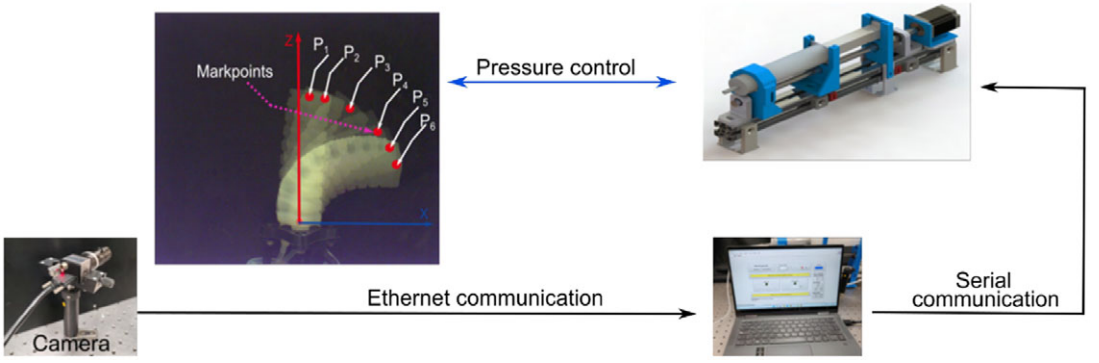

Figure 8. *Experiment assembly for module's characterisation.*

pressure, displacements (angular and linear) or the force that they can achieve to subsequently develop a type of control related to these variables.

Figure 8 shows the experiment assembly to characterise the module's motion. The module is fixed to the bottom, two red circular marks were placed on the module, one on the top and the other on the bottom. We use the camera IDS UI-3240CP-HQ 1/ 1.8", with a resolution of 1280 × 1024 ppi at 60 fps. The marks are using as reference points to track the module and measure the movement based on the applied pressure values. We proposed to perform six tests (T1–T6) for the characterisation of the module motion, and the six tests were averaged. Likewise, we developed a closed-loop FUZZY pressure control based on a piston, a cylinder, a worm gear and a stepper motor, as well as its user interface in LabVIEW.

The presented actuator addresses a wide mobility range since bending is performed in several directions. When a single channel is activated independently, the actuator generates bending in the four axes of Cartesian plane (X, Y). When activating two channels simultaneously, the bending is achieved in four different quadrants, and when three channels are activated at the same time, the bending motion is also performed in the four quadrants of Cartesian plane but with different curvature radius. Before performing the actuator's characterisation, three bending tests were performed to break the hysteresis [35].

We develop an application in Matlab to evaluate the bending angle at different pressure values. The methodology to compute the arc angle consists of capturing an image when the actuator has reached the applied pressure value. Subsequently, the image is inserted into the programme and with a tool we select the centres of the actuator's circular marks. In this way, Matlab obtains the coordinates of the point of interest, and we compute the curve radius with the Eq. (14) and $r = \frac{1}{k}$, [22] for each coordinate of the mark, where k is the inverse of the curvature radius r and X, Y, and Z are the position of the circle mark:

$$k(x, y, z) = \frac{2\sqrt{x^2 + y^2}}{x^2 + y^2 + z^2} \tag{14}$$

https://doi.org/10.1017/S026357472300067X Published online by Cambridge University Press

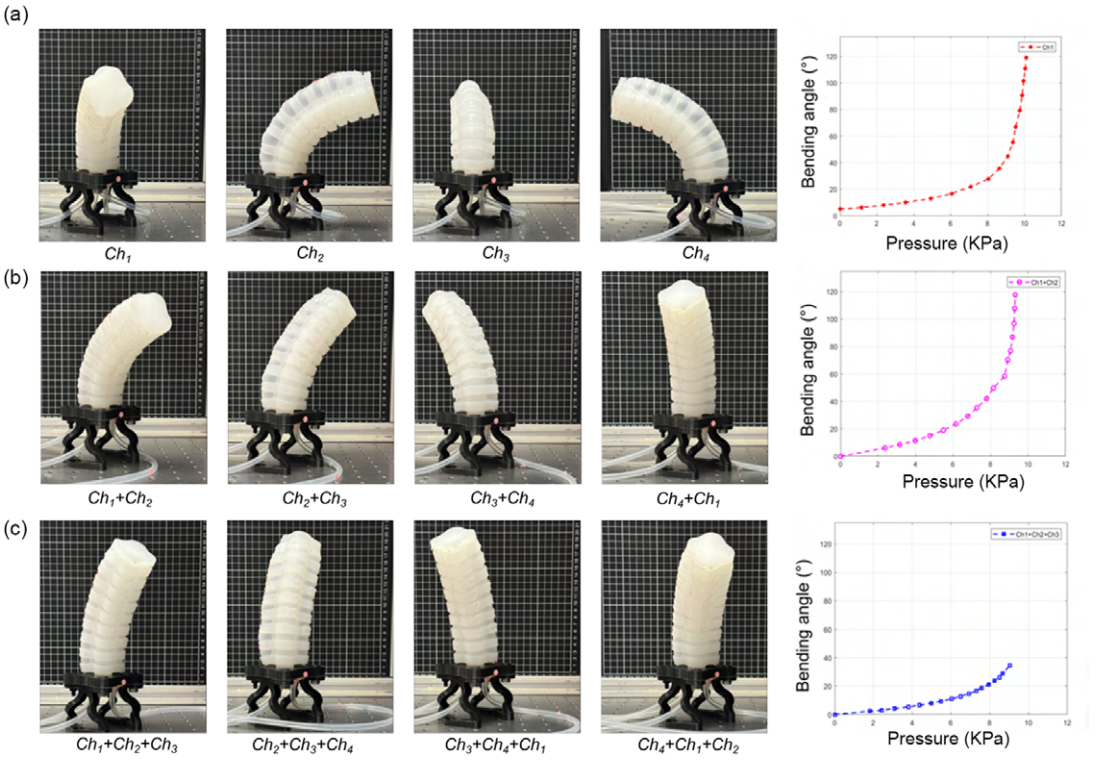

Figure 9. *Bending motion in different directions depending on the activation of: a) one channel, b) two channels and c) three channels.*

We evaluated the value k and the coordinates of the interest points (in a pressure value) in Eq. (13) to compute θ. This process is repeated for each desired pressure value.

The bending motion characterisation is presented for the independent activation of channel 1 (Ch_1), the simultaneous activation of channels 1 and 2 ($Ch_1 + Ch_2$), and the synchronised activation of channels 1, 2 and 3 ($Ch_1 + Ch_2 + Ch_3$). The distribution of the channels is shown in Fig. 1(b). The rest of the combination has the same bending angles but in different directions, as illustrated in Fig. 1(c). Figure 9 illustrates the mobility of the actuator in different direction according to the activation of the channel: (a) activation of a single channel, (b) synchronous activation of two channels and (c) simultaneous activation of three channels.

Figure 10(a) shows the graphics for the bending angle (°) vs pressure (kPa) related to the characterisation for Ch_1, $Ch_1 + Ch_2$ and $Ch_1 + Ch_2 + Ch_3$. In addition, we obtained a maximum angle of 123.95° at 10.19kPa when Ch_1 is activated independently. For the simultaneous activation of Ch_1 and Ch_2, the resulting bending angle was 115° for a pressure value of 9.32kPa; we achieved a bending angle of 28.91° by applying a pressure of 9.04kPa when activating the $Ch_1 + Ch_2 + Ch_3$, simultaneously.

Furthermore, the graphic in Fig. 10(b) shows different views of the angular and Cartesian relationship when are pressurised channels Ch_1 (right) and Ch_2 (left) independently. Likewise, Fig. 10(c) shows the angular trajectory and Cartesian relationship when we simultaneously activate channels $Ch_1 + Ch_2$ (right) and channels $Ch_2 + Ch_3$ (left).

4. Soft manipulator

4.1. Soft manipulator description and kinematics analysis

In order to demonstrate the impact of the proposed soft module, we developed a soft manipulator manufactured with the elastomer Ecoflex 00-50, one of the most commonly used materials in soft robotics.

https://doi.org/10.1017/S026357472300067X Published online by Cambridge University Press

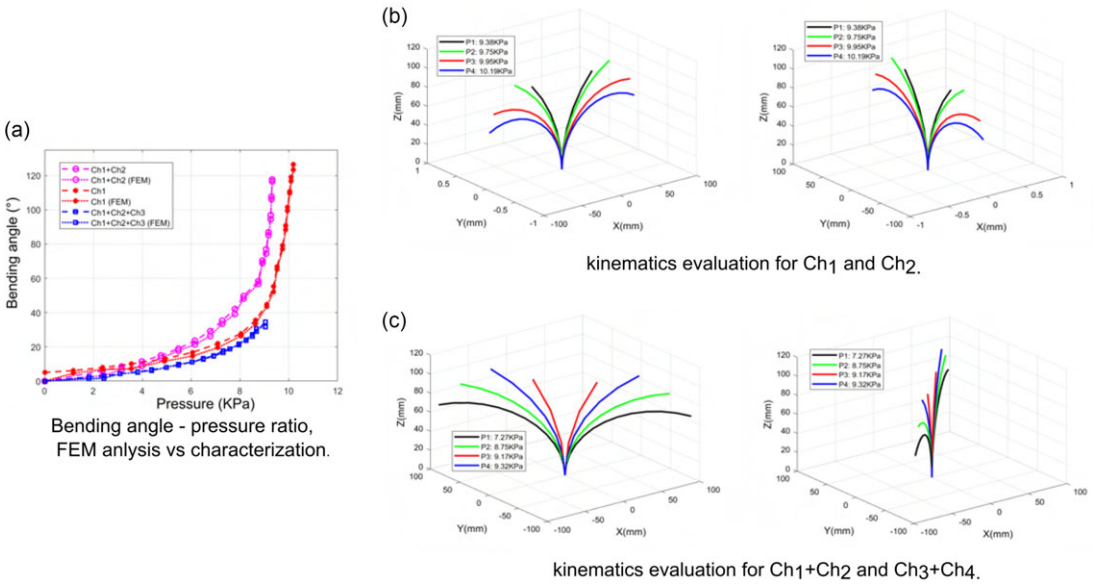

Figure 10. *Bending–angle vs pressure relationship for the activation of channels* Ch_1, $Ch_1{+}Ch_2$ *y* $Ch_1{+}Ch_2{+}Ch_3$.

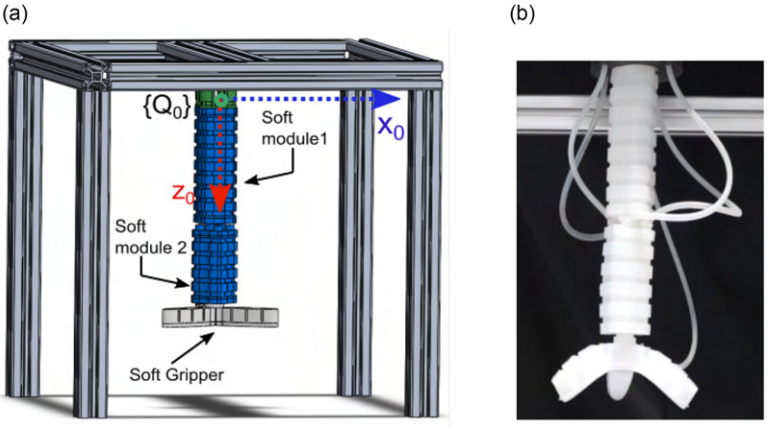

Figure 11. *Description of the soft manipulator. a) CAD design. b) Manufactured soft manipulator.*

The proposed manipulator consists of three completely soft elements, as shown in Fig. 11, two bending modules, and a soft gripper as end effector.

The length of modules one and two is 123 and 78 mm, respectively. Both modules have a width of 47 mm. The end effector consists of three fingers spaced at 120°. Through a single channel, it can open or close the fingers. Each one is designed with four chambers with a length of 65 mm and a height of 19 mm as shown in Fig. 12(a). For the manufacturing of the soft manipulator shown in Fig. 12(b), we assembled both models and the gripper by using the bonding method [36]. This method allows fusing two or more elements simply by first adding a thin layer of uncured material, similar to glue, and then finishing the curing process, the pieces accordingly stick together.

The robot has two non-deformable or "death-sections" due to the manufacturing process. The eight independent channels can be actuated with compressed air, where the position and orientation can be controlled by programmed pressure.

https://doi.org/10.1017/S026357472300067X Published online by Cambridge University Press

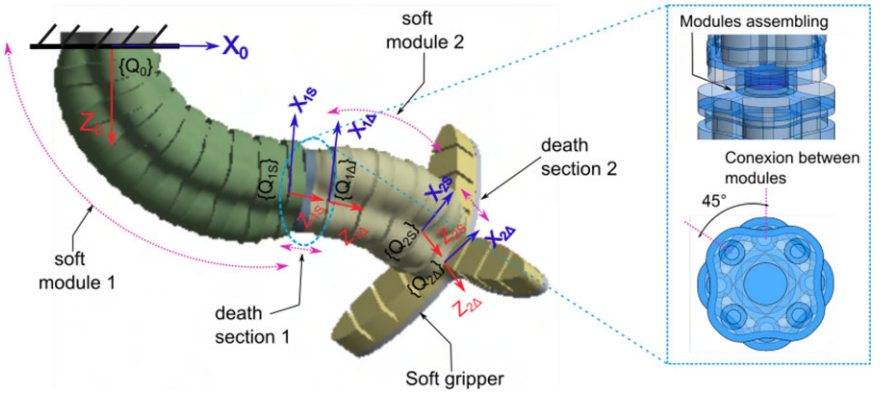

Figure 12. *Morphology of the bending modules and the end effector.*

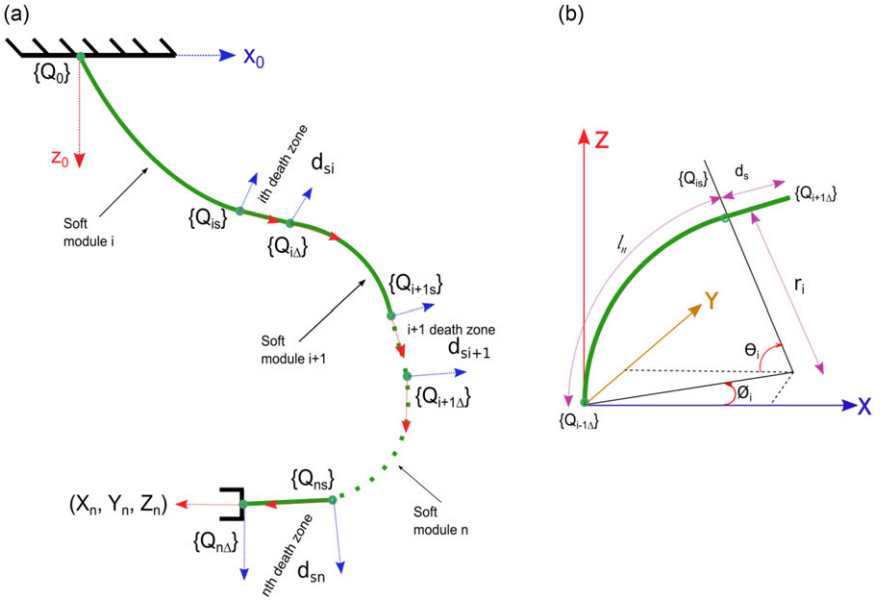

Figure 13. *Kinematics modelling: (a) Diagram of transform of the $i-th$ module position parameters (X_i, Y_i, Z_i) using length parameters (l_i) via arc parameters (k_i, ϕ_i, θ_i). (b) General kinematics model for a single bending module related to the curvature k.*

The proposed soft manipulator is shaped by two modules which bend continuously. Previous studies [29, 37] have already shown how to solve the forward transformation. The kinematic modelling describes the transformation from the channel's length (l_{ij}) to the coordinate of the end of the soft manipulator (X_n, Y_n, Z_n), where i and j represent the segment and channel, respectively (see Fig. 13(a)). Furthermore, Fig. 13(b) presents the general kinematics model for a single bending module, where r_i represents the curvature radius while l_i is the arc length of the $i-th$ channel.

Based on the work presented in ref. [29], we assume: (a) the curvature rate is constant in both bending module while the non-deformable section presents a line; (b) the channels of each bending segment are parallel, and the cross sections are equal in the same module; (c) the soft manipulator is analysed without gravity forces and load.

Taking into account those assumptions, we managed to simplify the soft manipulator kinematics as independently controlled constant curves. Figure 13(a) shows the transformation between n bending

https://doi.org/10.1017/S026357472300067X Published online by Cambridge University Press

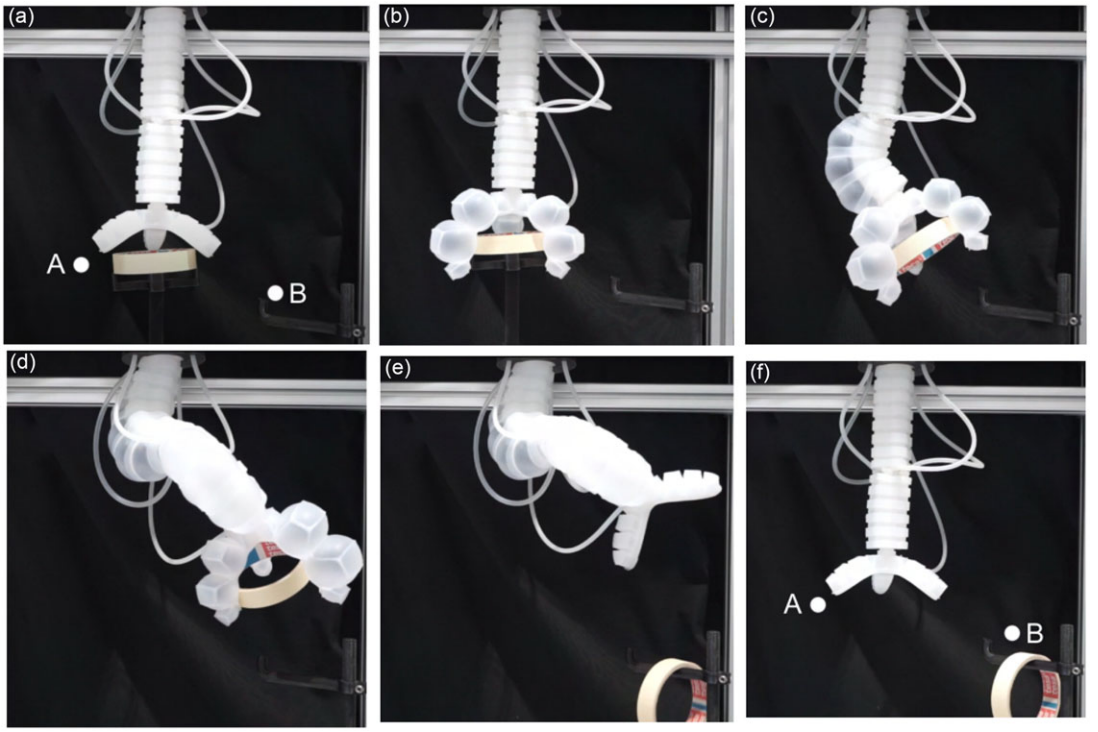

Figure 14. *Sequence images of a pick and place task.*

modules. Q_0 is the base static coordinate system, while Q_{is} and $Q_{i\triangle}$ represent the end of a bending module and a death section in the $i-th$ module.

Considering all the modules are actuated in the same way and the kinematics model of a single bending module derived in the previous section, we can figure out the transformation in a single module. The translation of the *ith* bending module regarded to curvature l_n can be represented as a rotation around the Y-axis with curvature angle θ_i. Rotation around the Z-axis is represented by φ_i as shown in Fig. 5. We consider that the X-axis points to the centre of the circle and that the Z-axis coincides with the tangent of the circle. Thus, multiplying the homogeneous matrix (which is constituted by a matrix of rotation and position) with the rotation matrix $R(\phi_i)$ and zero translation, we obtain the transformation matrix for one bending soft module:

$$T_{is}^{i-1\triangle} = \begin{bmatrix} c^2\phi_i c\theta_i + s^2\phi_i & c\phi_i s\phi_i(c\theta_i - 1) & c\phi_i s\theta_i & rc\phi_i(1 - c\theta_i) \\ c\phi_i s\phi_i(c\theta_i - 1) & s^2\phi_i c\theta_i + c^2\phi_i & s\phi_i s\theta_i & rs\phi_i(1 - c\theta_i) \\ -c\phi_i s\theta_i & -s\phi_i s\theta_i & c\phi_i & rs\theta_i \\ 0 & 0 & 0 & 1 \end{bmatrix} \tag{15}$$

The death module's transformation matrix is represented by Eq. (16), where d_{si} is the length of the death section of the *ith* bending module.

$$T_{i+1\triangle}^{is} = \begin{bmatrix} 1 & 0 & 0 & 0 \\ 0 & 1 & 0 & 0 \\ 0 & 0 & 1 & d_{si} \\ 0 & 0 & 0 & 1 \end{bmatrix} \tag{16}$$

https://doi.org/10.1017/S026357472300067X Published online by Cambridge University Press

From the combination of n bending modules and death sections, we can deduce the transformation for the soft manipulator as is described in Eq. (17):

$$T^{0}_{2\triangle} = T^{0}_{1s} \cdot T^{1s}_{1\triangle} \cdot T^{1\triangle}_{2s} \cdot T^{2s}_{2\triangle} \tag{17}$$

4.2. Motion sequence for the soft manipulator

We performed a motion sequence to pick an object from point A and place it at point B. The eight independent channels are controlled (in open loop) by programmed pressure signals.

The manipulation sequence starts at the rest position, as shown in Fig. 14(a). In this position, the robot is posed over the object. Thus, the soft gripper is activated and holds the object, as illustrated in Fig. 14(b). Afterwards, the orientation of the soft manipulator is controlled by pressurising one channel in each bending module, keeping the gripper activated. The activation of channel 1 (Ch_1) of bending module 2, followed by the pressurisation of channel 4 (Ch_4) of bending module 1, results in the manipulator being positioned over the B point, as shown in Fig. 14(c) & (d). When the manipulator is located, the gripper is depressurised and the object is placed, as illustrated in Fig. 14(e). Finally, the soft manipulator returns to its rest position (Fig. 14(f)).

5. Conclusion

In this article, we reported the design, FEM simulations, fabrication, kinematic model and characterisation of a multi-DOF soft pneumatic module that achieves bending in several directions.

Through FEM simulations, we demonstrated the wide range of motion of the module, such as continuous curvatures, using the Ecoflex 00-50 material.

The authors propose to divide the manufacturing process into different steps. For this, we presented a detailed design of the moulds for the casting technique, resulting in an easy and practical fabrication process and a module of excellent quality. In contrast, other studies have shown complex fabrication processes and post-manufacturing steps, such as fibre reinforcement.

Moreover, we implemented a FUZZY control to activate the channels of the soft module in different combinations. We presented the characterisation of the bending motion via computer vision. Likewise, the maximum bending angles are 123.9°, 115° and 28.91° when a single channel is activated independently and when two or three channels are activated simultaneously, obtaining deformation values in the range of previously reported modules [19, 21–25]. Thus, the module exhibits excellent mobility.

The geometry of the module achieves continuous curvatures, since the multi-DOF soft module does not present squishing in the centre of the arc, as demonstrated in Section 3.1. Furthermore, the module exhibits high dexterity; it can accomplish different curvatures radius according to the activated channels, reaching several points in the workspace.

We derived a kinematic model for the multi-DOF soft module, which evaluates the data obtained during the characterisation of bending motion for several pressure values. We presented the angular and Cartesian relationship of different pressure values for the activation of the module channels.

Due to the mobility of the multi-DOF soft module, it competes directly with the performance of the previously reported multi-motion modules, highlighting that the module design optimises the material amount since the design allows eliminating the excess material, reducing costs and weight, as well as improving the performance of the module, contrary to other authors who propose modules designed by cylindrical geometries filled with an excess of material, compromising their mobility. The semicircular geometry of the four channels facilitates the simulation and the manufacturing process, as opposed to using the combination of chambers and channels or reinforcing fibres. The channel distribution increases the range of mobility compared to those modules with only three.

Additionally, we proposed a modular soft manipulator based on two multi-DOF soft modules, considering only bending motions. The kinematic model was carried out, considering arc parameters for n-modules, taking into account the kinematic model of a single module.

https://doi.org/10.1017/S026357472300067X Published online by Cambridge University Press

This soft robot was manufactured using Ecoflex-0050, one of the most reported materials in soft robotics applications. This material has an elongation at break of 980%, presenting high deformations.

Through the soft manipulator, we demonstrated the potential of the multi-DOF soft module. The robot performs picking and placing tasks, unlike other authors who only present experimentation of mobility, [7, 8]. On the other hand, the soft manipulator releases high deformations in the radial direction due to its low shore hardness and elevated elongation at break. In this sense, oscillations can occur during the motion. However, a single multi-DOF soft module presents good performance while moving. In future work, taking into account the experimental data obtained in this research, a mathematical approach to define trajectories will be proposed to describe different profile motions, such as developing the experimental dynamic model to estimate load capabilities in diverse positions. As well as, develop the mathematical model of the module that expresses the pressure as a function of the angle of deformation.

Author contributions. Authors 1, 2 and 4 developed the multi-DOF soft pneumatic module, as well as contributed to the writing of the paper. Author 3 designed and fabricated the soft manipulator robot as well as contributed to the writing of the paper.

Financial support. This research received no specific grant from any funding agency, commercial or not-for-profit sectors

Conflicts of interest. The authors declare no conflicts of interest exist.

Ethical standards. Not applicable under the heading.

References

[1] S. Kim, C. Laschi and B. Trimmer, "Soft robotics: A bioinspired evolution in robotics," *Trends Biotechnol.* **31**(5), 287–294 (2013).
[2] R. K. Katzschmann, A. D. Marchese and D. Rus, *Hydraulic Autonomous Soft Robotic Fish for 3d Swimming* (Springer International Publishing, Cham, 2016) pp. 405–420.
[3] R. F. Shepherd, F. Ilievski, W. Choi, S. A. Morin, A. A. Stokes, A. D. Mazzeo, X. Chen, M. Wang and G. M. Whitesides, "Multigait soft robot," *Proc. Nat. Acad. Sci.* **108**(51), 20400–20403 (2011).
[4] Z. Tang, J. Lu, Z. Wang, G. Ma, W. Chen and H. Feng, "Development of a new multi-cavity pneumatic-driven earthworm-like soft robot," *Robotica* **38**(12), 2290–2304 (2020). doi: 10.1017/S0263574720000284.
[5] J. Z. Ge, A. A. Calderón, L. Chang and N. O. Pérez-Arancibia, "An earthworm-inspired friction-controlled soft robot capable of bidirectional locomotion," *Bioinspir. Biomim.* **14**(3), 036004 (2019 feb).
[6] C. Branyan, C. Fleming, J. Remaley, A. Kothari, K. Tumer, R. L. Hatton and Y. Mengüç, "Soft snake robots: Mechanical design and geometric gait implementation," **In:** *2017 IEEE International Conference on Robotics and Biomimetics (ROBIO)* (December 2017) pp. 282–289.
[7] B. Zhang, C. Hu, P. Yang, Z. Liao and H. Liao, "Design and modularization of multi-dof soft robotic actuators," *IEEE Robot. Automat. Lett*. **4**(3), 2645–2652 (2019).
[8] A. D. Marchese and D. Rus, "Design, kinematics, and control of a soft spatial fluidic elastomer manipulator," *Int. J. Robot. Res*. **35**(7), 840–869 (2016).
[9] X. Zhang and A. Oseyemi, "A herringbone soft pneu-net actuator for enhanced conformal gripping," *Robotica* **40**(5), 1345–1360 (2022). doi: 10.1017/S0263574721001144.
[10] S. M. Hadi Sadati, Y. Noh, E. S. Naghibi, K. Althoefer and T. Nanayakkara, "Stiffness Control of Soft Robotic Manipulator for Minimally Invasive Surgery (mis) Using Scale Jamming," **In:** *Intelligent Robotics and Applications* (H. Liu, N. Kubota, X. Zhu and R. Dillmann, eds.) Springer International Publishing, Cham, 2015) pp. 141–151.
[11] P. Polygerinos, Z. Wang, K. C. Galloway, R. J. Wood and C. J. Walsh, "Soft Robotic Glove for Combined Assistance and at-home Rehabilitation," **In:** *Robotics and Autonomous Systems.* vol. 73 (Wearable Robotics, 2015) pp. 135–143.
[12] S. Davarzani, M. Ahmadi-Pajouh and H. Ghafarirad, "Design of sensing system for experimental modeling of soft actuator applied for finger rehabilitation," *Robotica* **40**(7), 2091–2111 (2022). doi: 10.1017/S0263574721001533.
[13] D. V., Dienno, Design and Analysis of a Soft Robotic Manipulator with Base Rotation, Master's thesis. The Pennsylvania State University, 2006).
[14] B. Mosadegh, P. Polygerinos, C. Keplinger, S. Wennstedt, R. F. Shepherd, U. Gupta, J. Shim, K. Bertoldi, C. J. Walsh and G. M. Whitesides, "Pneumatic networks for soft robotics that actuate rapidly," *Adv. Funct. Mater.* **24**(15), 2163–2170 (2014).
[15] J. Bishop-Moser, G. Krishnan, C. Kim and S. Kota, "Design of soft robotic actuators using fluid-filled fiber-reinforced elastomeric enclosures in parallel combinations," **In:** *2012 IEEE/RSJ International Conference on Intelligent Robots and Systems* (October 2012) pp. 4264–4269.
[16] T. Wang, L. Ge and G. Gu, "Programmable design of soft pneu-net actuators with oblique chambers can generate coupled bending and twisting motions," *Sens. Actuat. A: Phys.* **271**, 131–138 (2018).

[17] H. K. Yap, H. Ng and R. C.-H. Yeow, "High-force soft printable pneumatics for soft robotic applications," *Soft Robot.* **3**(3), 144–158 (2016). doi: 10.1089/soro.2016.0030.
[18] J. Bishop-Moser, G. Krishnan, C. Kim and S. Kota, "Design of Soft Robotic Actuators Using Fluid-Filled Fiber-Reinforced Elastomeric Enclosures in Parallel Combinations," **In:** *2012 IEEE/RSJ International Conference on Intelligent Robots and Systems* (2012), pp. 4264–4269. doi: 10.1109/IROS.2012.6385966.
[19] Y. Elsayed, V. Augusto, C. Lekakou, G. Tao, C. Saaj, T. Ranzani, M. Cianchetti and A. Menciassi, "Finite element analysis and design optimization of a pneumatically actuating silicone module for robotic surgery applications," *Soft Robot.* **1**(4), 255–262 (2014). doi: 10.1089/soro.2014.0016.
[20] F.-Y. Xu, F.-Y. Jiang, Q.-S. Jiang and Y.-X. Lu, "Soft actuator model for a soft robot with variable stiffness by coupling pneumatic structure and Jamming mechanism," *IEEE Access* **8**, 1–1 (2020). doi: 10.1109/ACCESS.2020.2968928.
[21] S. Mustaza, Y. Elsayed, C. Lekakou, C. Saaj and F. Jan, "Dynamic modeling of fiber-reinforced soft manipulator: A visco-hyperelastic material-based continuum mechanics approach," *Soft Robot.* **6**(3), 305–317 (2019). doi: 10.1089/soro.2018.0032.
[22] H. Abidi, G. Gerboni, M. Brancadoro, J. Fras, A. Diodato, M. Cianchetti, H. A. Wurdemann, K. Althoefer and A. Menciassi, "Highly dexterous 2-module soft robot for intra-organ navigation in minimally invasive surgery," *Int. J. Med. Robot. Comput. Assist. Surg.* **14**(1), e1875 (2018).
[23] D. Garcia, S. Ibrahim, B.-H. Cao and A. Raatz, "Design and Characterization of a 3D Printed Soft Pneumatic Actuator," **In:** *New Trends in Mechanism and Machine Science. EuCoMeS 2020*. Mechanisms and Machine Science, vol 89. Springer, Cham (2020). doi: 10.1007/978-3-030-55061-5_55
[24] A. Raatz, D. Garcia, E. Castillo Castaneda and Y. Sandoval-Castro, Robust 3D printed modular soft pneumatic actuator using origami concept for high contraction soft systems (2021).
[25] X. Zhang and O. Ivlev, "Simulation of Interaction Tasks for Pneumatic Soft Robots Using SimMechanics," **In:** *19th International Workshop on Robotics in Alpe-Adria-Danube Region (RAAD 2010)* (2010) pp. 149–154. doi: 10.1109/RAAD.2010.5524594.
[26] L. Guo, K. Li, G. Cheng, Z. Zhang, C. Xu and J. Ding, "Design and experiments of pneumatic soft actuators design and experiments of pneumatic soft actuators," *Robotica* **39**(10), 1806–1815 (2021). doi: 10.1017/S0263574720001514.
[27] B. Phillips, K. Becker, S. Kurumaya, K. Galloway, G. Whittredge, D. Vogt, C. Teeple, M. Rosen, V. Pieribone, D. Gruber and R. Wood, "A dexterous, glove-based teleoperable low-power soft robotic arm for delicate deep-sea biological exploration," *Sci. Rep.* **8**(1) (2018). doi: 10.1038/s41598-018-33138-y.
[28] P. Kulkarni, *Centrifugal Forming and Mechanical Properties of Silicone-Based Elastomers for Soft Robotic Actuators* (New Brunswick Rutgers, 2015). PP. 26.
[29] R. J. Webster and B. A. Jones, "Design and kinematic modeling of constant curvature continuum robots: A review," *Int. J. Robot. Res.* **29**(13), 1661–1683 (2010).
[30] H. Abidi, G. Gerboni, M. Brancadoro, J. Fras, A. Diodato, M. Cianchetti, H. Wurdemann, K. Althoefer and A. Menciassi, "Highly dexterous 2-module soft robot for intra-organ navigation in minimally invasive surgery," *Int. J. Med. Robot.* **14**(1), (2018 Feb). doi: 10.1002/rcs.1875 (Epub 05 December, 2017).
[31] H. K. Yap, J. C. H. Goh and R. C. H. Yeow, "Design and Characterization of Soft Actuator for Hand Rehabilitation Application," **In:** *6th European Conference of the International Federation for Medical and Biological Engineering* (I. Lackovic and D. Vasic, eds.) (Springer International Publishing, Cham, 2015) pp. 367–370.
[32] N. Tan, X. Gu and H. Ren, "Design, characterization and applications of a novel soft actuator driven by exible shafts," *Mech. Mach. Theory.* **122**, 197–218 (2018).
[33] P. Polygerinos, S. Lyne, Z. Wang, L. F. Nicolini, B. Mosadegh, G. M. Whitesides and C. J. Walsh, "Towards a Soft Pneumatic Glove for Hand Rehabilitation," **In:** *2013 IEEE/RSJ International Conference on Intelligent Robots and Systems* (November 2013) pp. 1512–1517.
[34] X. Lu, W. Xu and X. Li, "A soft robotic tongue mechatronic design and surface reconstruction," *IEEE/ASME Trans. Mechatron.* **22**(5), 2102–2110 (2017).
[35] W. Shi and G. L. Z. Chen, "Effects of the bulk compressibility on rubber isolator's compressive behaviors," *Adv. Mech. Eng.* **9**(5), 15 (2017).
[36] F. Ilievski, A. Mazzeo, R. Shepherd, X. Chen and G. Whitesides, "Soft robotics for chemists," *Angew. Chem. (International ed., in English)* **50**(8), 1890–1895 (2011).
[37] Z. Gong, Z. Xie, X. Yang, T. Wang and L. Wen, "Design, fabrication and kinematic modeling of a 3D-motion soft robotic arm," **In:** *2016 IEEE International Conference on Robotics and Biomimetics (ROBIO)* (2016), pp. 509–514. doi: 10.1109/ROBIO.2016.7866373.
[38] S. Joshi and J. Paik, "Multi-dof force characterization of soft actuators," *IEEE Robot. Automat. Lett.* **4**(4), 3679–3686 (2019).

Cite this article: I. Santacruz-Mondragon, X. Y. Sandoval-Castro, S. Ibrahim, M. Wiese, A. Raatz, M. F. Ruiz-Torres and E. Castillo-Castaneda (2023). "Design and characterisation of a multi-DOF soft pneumatic module", Robotica **41**, 2774–2788. https://doi.org/10.1017/S026357472300067X